CrystEngComm

Strongly Adhering ZnO Crystal Layer via Seed/buffer-free, Low-Temperature Direct Growth on a Polyimide Film Using Solution Process

Journal:	*CrystEngComm*
Manuscript ID	CE-ART-07-2020-000961.R1
Article Type:	Paper
Date Submitted by the Author:	22-Jul-2020
Complete List of Authors:	Shishino, Kazuyuki; Shinshu Daigaku; Toray Engineering Co Ltd Yamada, Tetsuya; Shinshu Daigaku, Center for Energy and Environmental Science Arai, Masao; Raytech,INC Ikeda , Munekazu; Toray Engineering Co Ltd Hirata, Hajime; Toray Engineering Co Ltd Motoi, Masashi; Toray Engineering Co Ltd Hatakeyama, Tatsuo; Toray Engineering Co Ltd Teshima, Katsuya; Shinshu University, Department of Materials Chemistry; Shinshu University, Center for Energy and Environmental Science

ARTICLE

Strongly Adhering ZnO Crystal Layer via Seed/buffer-free, Low-Temperature Direct Growth on a Polyimide Film Using Solution Process

Received 00th January 20xx,
Accepted 00th January 20xx

DOI: 10.1039/x0xx00000x

Kazuyuki Shishino [ae], Tetsuya Yamada [b], Masao Arai [d], Munekazu Ikeda [e], Hajime Hirata [e], Masashi Motoi [f], Tatsuo Hatakeyama [g], Katsuya Teshima [*bc]

ZnO is a functional material used as a thin-film device that is can have various applications in a sustainable society. Generally, a seed/buffer layer is considered necessary for the fabrication of ZnO crystal layers on substrates. Herein, we demonstrated direct growth of the ZnO crystal layer without any such layers. Using the liquid-phase method, randomly oriented, rod-like ZnO crystals were formed directly from the polyimide film. The study confirmed irregularities in nano-order at the surface of the film, where ZnO crystals are fixed on. These results suggest that the anchor effect contributes to direct growth. According to our findings, a seed layer is not required for fabricating the ZnO crystal layer film if polymer substrates are optimally treated. Omitting a seed layer would open new insight into practical use of ZnO. Simplification of the mass production process, improvement of functionalities, such as transparency and thickness, as electric devices are potential examples.

1. Introduction

Zinc oxide (ZnO) possesses a variety of functionalities, such as transparency in the visible light region, good conductivity at electron-doped state,[1] and relatively high biological compatibility.[2] ZnO can be prepared and grown at low temperatures.[3,4] Moreover, zinc, as raw material, is available at a low cost. Both low-cost production and high functionalities indicate that ZnO as a functional material is widely used in our sustainable society. For applicable uses, ZnO is usually prepared on substrates such as glass,[5-7] metal,[8-10] and metal oxides.[11-13] Polymers are another candidate for substrates for ZnO. They exhibit individual properties of cheaper, lighter, and more flexible than other substrates, and accordingly, they are adapted as a substrate for industrial evolution. In various reports about the fabrication of ZnO crystal layers on polymer substrates, seed layers and/or buffer layers were commonly introduced on substrates. Metals (chromium, gold)[14,15] and metal oxides (Al_2O_3, ZnO)[16] are the representative layer. As a result, they contribute to adequate bonding between ZnO and substrates and promote crystallographic characteristics of ZnO, including crystal size, thickness, and density.

Although the seed/buffer layers are effective for fabricating ZnO crystals, there are some challenges regarding device functionality. One issue is production cost. Seed/buffer layers are usually prepared by deposition processes, such as spin coating,[17] sputtering,[18] dip coating,[19] and electrodeposition.[20] In other materials, liquid-phase exfoliation is sometimes adopted to fabricate nanosheet films.[21,22] These processes require specific atmosphere and pressure conditions and special electrodes. As a result, the production process is complex, which contributes to an increase in time and speed cost.

To overcome the issues, we propose the removal of seed/buffer layers for the fabrication of ZnO crystal layers. Our design will contribute to the body of knowledge by skipping the deposition process, which will simplify the production, increase transparency in transparent conductive films, and decrease the thickness of the films. Polymers exhibit various physicochemical properties, such as insulation, (semi-)conduction, and biocompatibility. These physicochemical properties suggest that polymers can partially substitute the role of seed and/or buffer layers. Several reports about the direct growth of ZnO on metal substrates such as Si have been published.[23,24] However, they require a high-temperature process, which is not applicable to polymers due to their relatively low thermal stability. Therefore, we assumed that the direct growth of ZnO should involve heterogeneous nucleation of ZnO on substrates. More precisely, we expected the preparation of the appropriate surface on the polymer, while the nucleation field of ZnO is taken into account.

[a.] *Graduate School of Medicine, Science and Technology, Shinshu University, 4-17-1 Wakasato, Nagano 380-8553, Japan*
[b.] *Research Initiative for Supra-Materials, Shinshu University, 4-17-1 Wakasato, Nagano 380-8553, Japan.*
[c.] *Department of Materials Chemistry, Faculty of Engineering, Shinshu University, 4-17-1 Wakasato, Nagano 380-8553, Japan*
[d.] *Production Dept, Production Team, Raytech, INC, 2-19-2 Nakadai, Kawagoe-City, Saitama, Japan*
[e.] *Research & Development Div, Toray Engineering Co., Ltd., 1-1, Sonoyama 1-chome, Otsu, Shiga, Japan.*
[f.] *Development Team, Business Div. Ⅱ, Mechatronics & Fine Technology Business Div, Toray Engineering Co., Ltd., 1-45, Oe 1-chome, Otsu, Shiga, Japan*
[g.] *Development Team, Business Div. Ⅰ, Mechatronics & Fine Technology Business Div, Toray Engineering Co., Ltd., 1-45, Oe 1-chome, Otsu, Shiga, Japan*
[*] Corresponding author's email: teshima@shinshu-u.ac.jp
†Electronic Supplementary Information (ESI) available: Surficial EDS spectra of Kapton and the fabricated product. See DOI: 10.1039/x0xx00000x

In this study, we demonstrated the fabrication of ZnO crystal layers on a polyimide substrate without any seed/buffer layer among them. A solution method was adopted for the fabrication. We assumed that the continuous supply of raw material from the solution leads to a smooth formation and growth of ZnO crystal layers at low temperatures. Surficial and cross-sectional characteristics of the fabricated thin film were examined in terms of chemical composition, elements, and shape. These results are considered regarding the surficial properties of the polymer and formation and growth manner of ZnO to discuss a bonding manner at the ZnO-polyimide interface.

2. Experimental

2.1 Fabrication of ZnO crystal layers on the polyimide film

We used polyimide as a polymer substrate due to its high plasticity and thermal stability. The material was Kapton as one of the representative polyimides (Kapton Type VN Film, DU PONT-TORAY CO., LTD.). We call the material as polyimide, afterward. The preparation procedure included the following four steps. STEPS 1-3 consisted of the surface treatment of polyimide film, and STEP 4 was the fabrication of ZnO crystal layers.

STEP 1 Alkali treatment of polyimide film

For the alkali treatment, the polyimide film was immersed in the following liquids:
(I) An aqueous solution made of 12 g/L $KMnO_4$ (99 %, Kanto Chemical Co., Inc.) and 4 g/L NaOH (95 %, Kanto Chemical Co., Inc.) at 80 °C for 5 min.
(II) To neutralize alkali, an aqueous solution made of 7 g/L hydroxylamine hydrochloride (96 %, Kanto Chemical Co., Inc.) at 40 °C.
(III) H_2SO_4 (98 %, MC FERTICOM Co., Ltd.) solution at 40 °C.
Finally, the immersed polyimide film was washed by water, blown off the dropping, and then dried in an oven at 60 °C for 15 min.

STEP 2 Plasma treatment of polyimide film

Plasma treatment (SAMCO Inc, PC-1000) was performed at 500 W for 300 s in vacuum condition at 10 Pa. Vacuum condition was made by exhausting air and exchanged by Ar for several times.

STEP 3 Heat treatment of polyimide film

Heat treatment was performed at 400 °C for 3 h in total, including heating and holding processes. After the heating, the film was naturally cooled down to room temperature.

STEP 4 Fabrication of ZnO crystal layers

ZnO crystal layers were fabricated on the surface-treated polyimide film using a dip coating method referring to the previous report,[25] except for the use of a Cr intermediate layer. A 30 mM $Zn(NO_3)_2{\cdot}6H_2O$ (44.57 g, 99 %, Alfa Aesar.com) solution was added into 5 L of pure water heated to 50 °C and mixed by stirring for 5 min. Then, 21.13 g of 30 mM hexamethylenetetramine (HMT) (99 %, FUJIFILM Wako Pure Chemical Corp.) was added to be mixed for 5 min. The surface-treated polyimide film was immersed in this solution and heated at 90 °C for 3 h. The product was put out and washed with hot water at 70 °C for 1 min to remove extra reactants on the film. After being blown off the water, the film was dried in an oven at 60 °C for 15 min.

2.2 Characterization

The chemical phase was examined using X-ray diffraction (XRD, Rigaku Corporation, Miniflex600). The measurement was performed in the 2θ region between 10° and 80° region with a Cu Kα radiation (λ = 0.154 nm) with a scan speed of $10°{\cdot}min^{-1}$ and a resolution of 0.02°. The surface shape of the thin film was observed using a field emission scanning electron microscope (FESEM, JEOL Ltd., JSM-7600F). Depositing Pt by electron sputtering, the sample was measured at an acceleration voltage of 15 kV. The elemental composition of the product was analysed using an energy dispersive X-ray spectrometer (EDS, Thermo Fisher Scientific Inc., Ultra Dray) at an acceleration voltage of 15 kV in an energy range between 0 and 20 keV. The cross-sectional shape and elemental composition mapping were investigated at Toray Research Center, Inc. Sliced samples for cross-sectional analyses were prepared by focused ion beam (FIB, roughly cutting out by SMI3200SE, Seiko Instruments Inc., cutting out by FB 2000A, Hitachi, Ltd., and finishing by Strata400S, FEI Company). The polyimide film was covered by epoxy-type resin for subsequent observations. The cross-sectional shape was observed using a scanning transmission electron microscope (STEM, JEOL, JEM-ARM200F) at an accelerating voltage of 200 kV. The cross-sectional composition was analysed using EDS (JEOL, Centurio) attached to STEM.

3. Result and Discussion

3.1 Fabrication of the ZnO crystal layer on the polyimide film

We dipped the surface-treated polyimide film in a solution of $Zn(NO_3)_2$ and HMT. The appearance of the film did not change at 50 °C. During heating the solution to 90 °C, a white product was gradually formed on the film, and finally, it fully covered the polyimide film. This result indicates that some chemical reaction occurs in the film above 50 °C. Surficial morphology of the dip-coated product was investigated. Figure 1(a) shows a photographic image of this product and brown and white appearances [(I) and (II), respectively, in the figure]. The brown one should be at the raw polyimide film. This region was masked with tape during the dipping process and inhibited in contact with the aqueous solution. SEM image of the brown fraction did not exhibit a visible product on it, as illustrated in Figure 1(b). White solids are adhered to the entire surface except of outside the polyimide film. SEM image of the white solids exhibited rod-like crystals, uniformly and densely attached to the film in Figure 1(c). Figure 1(d) is the high-magnification image of Figure 1(c).
The rod-like crystals are sharp-pointed in length less than 1 μm for a short side and around 3 μm for a long side, and they are randomly oriented. Figure 1(e) shows the root of the rod-shaped crystal seen at the boundary between [I] and [II] in

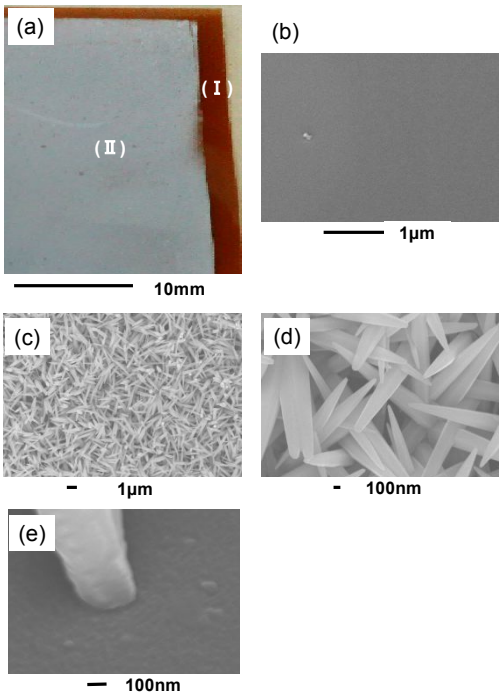

Fig.1 (a) Photographic image of the fabricated product. (b) SEM images of the brown part at (I) in (a), and (c) the white part at (II) in (a). (d) high-magnification image of the white part at (II) in (a). (e) Interface between ZnO crystal root and polyimide layer.

Figure 1(a). There are no apparent intermediate layers, such as seed and binder layers, between them, indicating their direct bonding. Figure 2 shows the XRD profile of the fabricated product. For comparison, XRD profiles of raw polyimide film and reference data of ZnO [Crystallography Open Database (COD) 1011258] are also shown. The XRD patterns of the product are composed of only polyimide and ZnO. Figure S1 in Electronic Supplementary Information (ESI) shows the surficial EDS spectrum of the product. There are elemental components of carbon, oxygen, zinc, and platinum. Pt is derived from sputtering deposition, while other elements should be derived from ZnO and polyimide. These results indicate that the fabricated product does not possess composition, except for ZnO and polyimide. Afterward, we called the product the ZnO crystal layer.

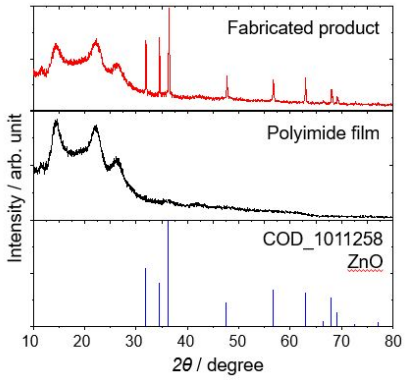

Fig.2 XRD profiles of the fabricated product, raw polyimide film, and reference of ZnO [Crystallography Open Database (COD) 1011258].

Next, the cross-sectional state of the crystal layer was examined to understand the interfacial bonding between ZnO and polyimide. Figures 3 (a) (b) illustrate a cross-sectional high angle annular dark field (HAADF) STEM images of the ZnO crystal layer. Hexagonal rod-like crystals with bright contrast were randomly oriented at the upper part of the images. Considering that the contrast depends on the atomic number in the HAADF-STEM image, the crystals can be assigned to ZnO, whereas the dark base is attributed to polyimide. Figure 3(c) shows the EDS elemental mapping of the image in Figure 3(b). Each image corresponds to maps of carbon (red), nitrogen (green), oxygen (yellow), and zinc (pink) in this order. The rod crystal is composed of oxygen and zinc elements, while carbon, nitrogen, and oxygen elements were detected in the base. These results also imply the existence of ZnO and polyimide, respectively and support our identification. Nitrogen element was detected in the surrounding of ZnO crystals, probably derived from epoxy-type resin and its curing agent. The contrast of HAADF-STEM image and elemental mapping were drastically changed at the interface of the ZnO and polyimide. Line elemental analysis was performed to understand the interface in detail, as illustrated in Figure 3(d). The elemental scanning direction was from a rod-like crystal of ZnO to polyimide film, as in Figure 3(b). Atomic percent of zinc is almost constant in the

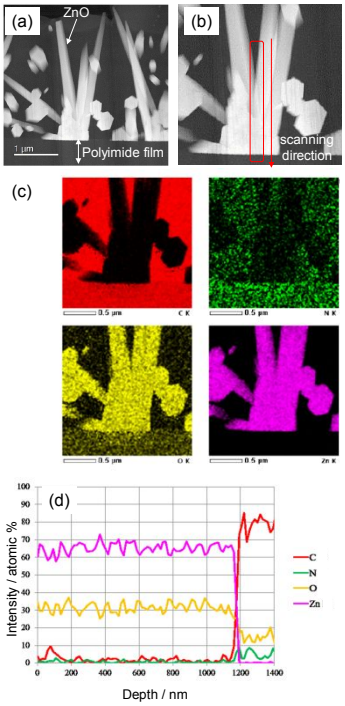

Fig.3 (a) low-magnification and (b) high-magnification HAADF-STEM images, and (c) elemental mapping images of the ZnO crystal layer. Each image corresponds to carbon (red), nitrogen (green), oxygen (yellow), and zinc (pink), in this order. (d) Line elemental mapping of carbon (c), nitrogen (N), oxygen (O), and zinc (Zn) in the line direction indicated in the HAADF-STEM image of (b).

region of the rod-like crystal, and a rapid decrease of zinc was found at the interface between the crystal and polyimide, as in Figure 3(d). The atomic percent of Zn and O are deviated from the stoichiometric value of ZnO. The characteristic X-rays of the light element (O) are absorbed by the heavy element (Zn) due to the nature of the EDX analysis, and the detection amount is reduced. Therefore, the quantitative value of (O) is underestimated. Considering that XRD did not identify any other components except the composition of ZnO and polyimide, result suggests that there is no intermediate layer at the interface, and ZnO crystals directly attach to the polyimide film.

The random orientation and direct growth of ZnO crystals from polyimide film was further investigated to understand the origin. Figure 4 shows a bright-field scanning transmission electron microscopic (BF-STEM) image of the interface between ZnO (black portion) and polyimide (white base). The high-magnification image exhibits less than 100 nm of periodic irregularities at the surface of the polyimide film, where ZnO crystals lie on. Moreover, the grain boundary was found in ZnO crystals, as indicated by a dashed line. This means that individual ZnO crystals are stack one after another. Figure 4(b) focuses on the edge of ZnO crystals on the polyimide film. The concave portion of the polyimide film appears at the end of the ZnO crystals. This morphologic characteristic suggests that ZnO crystals are fixed directly on the polyimide film by an anchor effect.

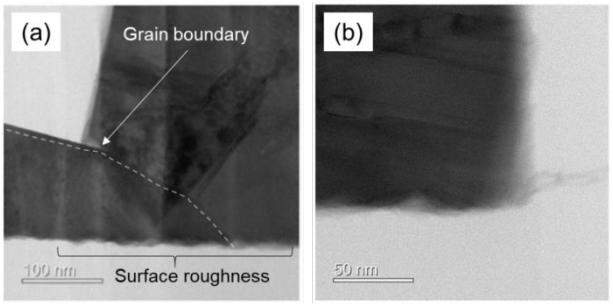

Fig.4. BF-STEM image of the interface between ZnO and P polyimide at (a) the grain boundary and (b) the edge of ZnO crystals. Dashed line in (a) indicates the grain boundary of the crystals.

3.2 Fabrication manner of the ZnO crystal layer on the polyimide film

Based on the experimental results, the fabrication manner of the ZnO crystal layer on the polyimide film is discussed. It is assumed that formation and crystal growth of ZnO involves the thin film formation, as illustrated in Figure 5 as follows.

Step 1: Formation of irregularities on the surface of the polyimide film

Surficial treatments of the polyimide film form the surficial irregularities in several nano decades. It is established that treatments by alkali, vacuum plasma, and heat remove impurities, including oils, fats, and organic substances. Additionally, the surficial treatments changed the morphology of the polyimide, probably due to chemical effects, such as hydrophilization, iridizations in the amide functional group, and/or dehydration. These processes should accompany surface activation of the film.

Step 2: Nucleation of ZnO on the polyimide film

In the early stage of heating from 50 °C to 90 °C, nucleation of ZnO or its derivative should occur on the surface of the polyimide film in a heterogeneous nucleation manner. When ZnO or its derivative in solution are transported and collided on the polyimide, they should be adhered at the micro-asperity of polyimide film surface. The fine irregularities of the polyimide work at this step surface and facilitate nucleation on this film. In addition, chemical adsorption might involve, as it is expected, that the activated surface of the polyimide facilitates chemical bonding with ZnO.

Step 3: Growth of ZnO crystals on the polyimide film

In the late stage on the heating to 90 °C, ZnO nuclei grow into sharp, pointed hexagonal crystal rods by feeding raw materials from solution. ZnO possesses a hexagonal wurtzite-type crystal structure. Derived from this anisotropic structure, ZnO is known to exhibit crystal shapes of the od, plate type with various aspect ratios.[26] The rod-like crystal shape of ZnO has been already reported to facilitate growth direction [0001] in a hexagonal crystal system, reflecting larger surface energy at (0001) crystal surface than at other planes.[27] The rod-like ZnO crystals in this study should also grow to an equilibrium form comparable to the references. The concave region was found at the polyimide film, where ZnO crystals are fixed, as in Figure 4(b). It is assumed that this morphology was induced from compression stress by nucleation and subsequent crystal

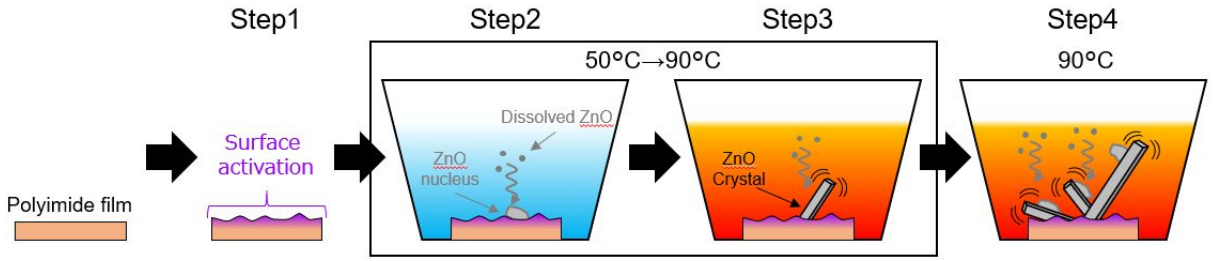

Fig.5. Schematic views of the fabrication manner of the ZnO crystal layer on the polyimide film.

growth of ZnO on the polyimide. A combination of the compression stress and the periodic irregularities of the polyimide film would be a primary factor leading to the anchor effect. Alternatively, it is possible that certain chemical interactions form rigid interfacial bonds. For example, some functional groups on the polyimide surface may interact with ZnO.

Step 4: Repeatable nucleation and crystal growth of ZnO

During the temperature holding at 90 °C, the formation and crystallization of ZnO are facilitated. In this condition, critical nucleation of ZnO may occur in a solution as a homogeneous manner; then they sequentially fall down onto both the ZnO crystal layer and the polyimide film. By supplying the reactants from raw material solution, ZnO nucleation and subsequent crystallization occur repeatably on polyimide and ZnO. As a result, dense, rod-like ZnO crystal groups are formed on the polyimide films. Each ZnO crystal was randomly oriented. It is assumed that the nuclei of ZnO grow in a random direction, as the polyimide has no impact on controlling a growth direction in both chemical and physical aspects.

Conclusions

We demonstrated the growth of ZnO on a polyimide film and investigated its bonding manner. Surface- treated polyimide film were dipped in a solution of $Zn(NO_3)_2$ and HMT. Single-phase ZnO formed to fully cover the film at 90 °C. The morphology of the ZnO crystals was confirmed to be rod-like in size less than 1 μm for the short side and about 3 μm for the long side, and they are homogeneously stacked on the polyimide film in random orientations. Cross-sectional elemental and composition analyses did not reveal an intermediate layer at the interface between ZnO and the polyimide film, and the ZnO crystals were deposited on the polyimide film with about 100 nm of periodic irregularities. These results indicate that ZnO crystals were grown directly from the polyimide surface by the anchor effect. We also assume chemical effects might facilitate the immobilization. Significance of our finding is the possible fabrication of ZnO on a flexible film without any seed or buffer layer.

There are still various issues to be solved, including the surficial state of polyimide, characteristics of chemical bonding between ZnO and polyimide, and their origins. We plan to clarify these issues in our next report.

Conflicts of interest

The authors declare no competing financial interest.

Acknowledgements

This work was partially supported by JST Program on Open Innovation Platform with Enterprises, Research Institute and Academia JPMJOP1843, and JST Center of Innovation, Young Collaborative Research Fund, Digital Field R1WD12.

Notes and references

1 D. S. Bhachu, G. Sankar, I. P. Parkin, Aerosol Assisted Chemical Vapor Deposition of Transparent Conductive Zinc Oxide Films, *Chem. Mater.* 2012, **24**, 4704−4710.
2 A. Moezzi, A. M. McDonagh, M. B. Cortie, Zinc oxide particles: Synthesis, Properties and Applications, *Chem. Eng. J.* 2012, **185-186**, 1–22.
3 X. Wu, L. Zheng, D. Wu, Fabrication of Superhydrophobic Surfaces from Microstructured ZnO-Based Surfaces via a Wet-Chemical Route, *Langmuir* 2005, **21**, 2665-2667.
4 M. Lai, D. J. Riley, Templated Electrosynthesis of Zinc Oxide Nanorods, *Chem. Mater.* 2006, **18**, 2233-2237.
5 X. Yan, Z. Li, R. Chen, W. Gao, Template Growth of ZnO Nanorods and Microrods with Controllable Densities, *Cryst. Growth Des.* 2008, **8**, NO.7, 2406–2410.
6 X. Yan, Z. Li, C. Zou, S. Li, J. Yang, R. Chen, J. Han, W. Gao Renucleation and Sequential Growth of ZnO Complex Nano/Microstructure: From Nano/Microrod to Ball-Shaped Cluster, *J. Phys. Chem. C* 2010, **114**, 1436–1443.
7 Z. Lu, H. Xu, M. Xin, K. Li, H. Wang, Induced Growth of (0001)-Oriented Hydroxyapatite Nanorod Arrays on ZnO-Seeded Glass Substrate, *J. Phys. Chem. C* 2010, **114,** 820–825.
8 J. Song, S. Lim, Effect of Seed Layer on the Growth of ZnO Nanorods, *J. Phys. Chem. C* 2007, **111**, 596-600.
9 M. Chen, C. Pan, T. Zhang, X. Li, R. Liang, Z. L. Wang, Tuning Light Emission of a Pressure-Sensitive Silicon/ZnO Nanowires Heterostructure Matrix through Piezo-phototronic Effects, *ACS Nano* 2016, **10**, 6074−6079.
10 Y. Wei, W. Wu, R. Guo, D. Yuan, S. Das, Z. L. Wang, Wafer-Scale High-Throughput Ordered Growth of Vertically Aligned ZnO Nanowire Arrays, *Nano Lett.* 2010, **10**, 3414–3419
11 S.H. Lee, S.H. Han, H. S. Jung, H. Shin, J. Lee, J.H. Noh, S. Lee, I.S. Cho, J.K. Lee, J. Kim, H. Shin, Al-Doped ZnO Thin Film: A New Transparent Conducting Layer for ZnO Nanowire-Based Dye-Sensitized Solar Cells, *J. Phys. Chem. C* 2010, **114**, 7185–7189
12 W. Peng, S. Qu, G. Cong, Z. Wang, Synthesis and Structures of Morphology-Controlled ZnO Nano- and Microcrystals, *Cryst. Growth Des.* 2006, **6**, NO.6, 1518-1522.
13 D. Lee, K. Yong, Superstrate CuInS2 Photovoltaics with Enhanced Performance Using a CdS/ZnO Nanorod Array, *ACS Appl. Mater. Interfaces* 2012, **4**, 6758−6765.
14 S, Joshi, M. M. Nayak, K. Rajanna, Evaluation of Transverse Piezoelectric Coefficient of ZnO Thin Films Deposited on Different Flexible Substrates: A Comparative Study on the Vibration Sensing Performance, *ACS Appl. Mater. Interfaces* 2014, **6**, 7108−7116.
15 M. Ryu, J. H. Yang, Y. Ahn, M. Sim, K. H. Lee, K. Kim, T. Lee, S.J. Yoo, S. Y. Kim, C. Moon, M. Je, J.W. Choi, Y. Lee, J. E. Jang, Enhancement of Interface Characteristics of Neural Probe Based on Graphene, ZnO Nanowires, and Conducting Polymer PEDOT, *ACS Appl. Mater. Interfaces* 2017, **9**, 10577−10586.
16 W. W. Lee, J. Yi, S. B. Kim, Y.H. Kim, H.G. Park, W. I. Park, Morphology-Controlled Three-Dimensional Nanoarchitectures Produced by Exploiting Vertical and In-Plane Crystallographic Orientations in Hydrothermal ZnO Crystals, *Cryst. Growth Des.* 2011, **11**, 4927–4932.
17 O. H. Kwon, J. W. Jang, S.J. Park, J. S. Kim, S. J. Hong, Y. S. Jung, H. Yang, Y. J. Kim, Y. S. Cho, Plasmonic-Enhanced Luminescence Characteristics of Microscale Phosphor Layers on a ZnO Nanorod-Arrayed Glass Substrate, *ACS Appl. Mater. Interfaces* 2019, **11**, 1004−1012.
18 C. Li, G. Fang, J. Li, L. Ai, B. Dong, X. Zhao, Effect of Seed Layer on Structural Properties of ZnO Nanorod Arrays Grown by Vapor-Phase Transport, *J. Phys. Chem. C* 2008, **112**, 990-995.
19 S. Guillemin, E. Appert, H. Roussel, B. Doisneau, R. Parize, T, Boudou, G, Bremond, V. Consonni, Controlling the Structural

Properties of Single Step, Dip Coated ZnO Seed Layers for Growing Perfectly Aligned Nanowire Arrays, *J. Phys. Chem. C* 2015, **119**, 21694−21703.

20 Z. Zhang, G. Meng, Q. Xu, Y. Hu, Q, Wu, Z. Hu, Aligned ZnO Nanorods with Tunable Size and Field Emission on Native Si Substrate Achieved via Simple Electrodeposition, *J. Phys. Chem*. *C* 2010, **114**, 189**–**193.

21 Z. Li, H. Qiao, Z. Guo, X. Ren, Z. Huang, X. Qi, S. C. Dhanabalan, J. S. Ponraj, D. Zhang, J. Li, J. Zhao, J. Zhong, H. Zhang, High-Performance Photo-Electrochemical Photodetector Based on Liquid-Exfoliated Few-Layered InSe Nanosheets with Enhanced Stability, *Adv. Funct. Mater*. 2018, **28**, 1705237.

22 C. Xing, W. Huang, Z. Xie, J. Zhao, D. Ma, T. Fan, W. Liang, Y. Ge, B. Dong, J. Li, H. Zhang, Ultrasmall Bismuth Quantum Dots: Facile Liquid-Phase Exfoliation, Characterization, and Application in High-Performance UV−Vis Photodetector, *ACS Photonics* 2018, **5**, 621−629.

23 S. Vallejos, N. Pizúrová, I. Gràcia, C. S. Vazquez, J Čechal, C. Blackman, I. Parkin, C. Cané, ZnO Rods with Exposed {100} Facets Grown via a Self-Catalyzed Vapor−Solid Mechanism and Their Photocatalytic and Gas Sensing Properties, *ACS Appl. Mater. Interfaces* 2016, **8**, 33335−33342.

24 A. Jiamprasertboon, S. C. Dixon, S. Sathasivam, M. J. Powe, Y. Lu, T. Siritanon, C. J. Carmalt, Low-Cost One-Step Fabrication of Highly Conductive ZnO:Cl Transparent Thin Films with Tunable Photocatalytic Properties via Aerosol-Assisted Chemical Vapor Deposition, *ACS Appl*. Electron. Mater. 2019, **1**, 1408−1417.

25 T. Yasui, T. Yanagida, S. Ito, Y. Konakade, D. Takeshita, T. Naganawa, K. Nagashima, T. Shimada, N. Kaji, Y. Nakamura, I. A. Todorus, Y. He, S. Rahong, M. Kanai, H. Yukawa, T. Ochiya, T. Kawai, Y. Baba, Unveiling massive numbers of cancer-related urinary-microRNA candidates via nanowires, *Sci. Adv.* 2017, **3**, e1701133.

26 S. Kumar, H. J. Lee, T. H. Yoon, C. N. Murthy, J. S. Lee, Morphological Control over ZnO Nanostructures from Self-Emulsion Polymerization, *Cryst. Growth Des.* 2016, **16**, 3905−3911.

27 Z. L. Wang. Zinc Oxide Nanostructures: Growth, Properties and Applications, *J. Phys.: Condens. Matter.* 2004, **16**, R829–R858.

